BMB
Reports

BMB Rep. 2025; 58(2): 75-81
www.bmbreports.org

Wnt5a exacerbates pathological bone features and trabecular bone loss in curdlan-injected SKG mice via osteoclast activation

Min Whangbo[1,2,#], Eunae Ko[1,2,#], Dongju Kim[1,2], Chanhyeok Jeon[1,2], Hye-Ryeong Jo[1], Seung Hoon Lee[1], Jeehee Youn[3], Sungsin Jo[4,] & Tae-Hwan Kim[1,2,5,*]*

[1]Hanyang University Institute for Rheumatology Research (HYIRR), Seoul 04763, [2]Department of Translational Medicine Science, Graduate School of Biomedical Science and Engineering, Hanyang University, Seoul 04763, [3]Department of Anatomy & Cell Biology, College of Medicine, Hanyang University, Seoul 04763, [4]Department of Biology, College of Natural Sciences, Soonchunhyang University, Asan 31538, [5]Department of Rheumatology, Hanyang University Hospital for Rheumatic Diseases, Seoul 04763, Korea

Many studies on osteoblasts have suggested that Wnt5a plays a crucial role in excessive osteoblast activity, which is responsible for ectopic new bone formation, but research on osteoclasts in ankylosing spondylitis (AS) remains relatively limited. This study aimed to explore whether Wnt5a influences osteoclast-mediated bone resorption in curdlan-injected SKG mice, a model that mimics AS. Compared to the Vehicle group, the Wnt5a treatment group exhibited statistically higher clinical arthritis scores and increased hindpaw thickness values. Micro–computed tomography (microCT) analysis of hindpaws revealed a significant increase in inflamed and ectopic bone density in the Wnt5a-treated group compared to the Vehicle group. Histological examination also showed pronounced inflammation and structural bone damage in the bone marrow of ankles in the Wnt5a-treated group. Intriguingly, microCT analysis of the femur revealed that trabecular bone loss was markedly observed in the Wnt5a-treated group. Both the number of TRAP-positive osteoclasts and their activity were statistically greater in the Wnt5a-treated group compared to the Vehicle group. Serum markers of bone resorption, but not bone formation, were also significantly elevated in the Wnt5a-treated group. Notably, promotion of osteoclast differentiation by Wnt5a was inhibited following treatment with anti-Wnt5a. These findings suggest that targeting Wnt5a could be a promising strategy for mitigating pathological bone features in AS by modulating osteoclast activity. [BMB Reports 2025; 58(2): 75-81]

INTRODUCTION

Ankylosing spondylitis (AS) is a chronic inflammatory disease that primarily affects the spine and sacroiliac joints, potentially leading to excessive new bone formation and spinal ankylosis (1, 2). The pathogenesis of AS is characterized by chronic inflammation, which induces bone erosion at sites of local inflammation through osteoclast activity, followed by new bone formation mediated by osteoproliferation (3). Furthermore, clinical observations and animal model studies across several decades indicate that, while controlling inflammation is crucial for mitigating rapid disease progression, it may not be sufficient to fully block disease progression and ankylosis in AS.

Bone homeostasis is tightly regulated by complex interactions with osteoclast-mediated bone resorption and osteoblast-mediated bone formation. In AS, key pathways involved in osteoproliferation include bone morphogenetic proteins (BMPs) and Wingless-type signaling (Wnt) proteins, which are likely to play critical roles in ankylosis and may serve as potential therapeutic targets (4, 5). The activation of Wnt signaling pathways is crucial for the initiation of ectopic new bone formation by osteoblasts in AS (6). Although numerous studies on osteoblasts have provided insight into pathophysiological bone features in AS, research on osteoclasts in AS remains relatively limited.

Wnt5a, a member of the non-canonical WNT pathway, is known to play a significant role in both osteoclast-mediated bone resorption and osteoblast-mediated bone formation. Wnt5a is highly expressed in surgical bone tissues and associated with disease progression in AS (6). Intriguingly, it has been reported that the expression of Wnt5a was noticeably increased in calvaria Alkaline phosphatase (ALP)-positive cells, thereby enhancing osteoclast differentiation and activity in a collagen-induced arthritis mouse model (7). These findings

*Corresponding authors. Sungsin Jo, Tel: +82-41-530-4883; Fax: +82-41-530-1256; E-mail: joejo0517@sch.ac.kr; Tae-Hwan Kim, Tel: +82-2-2290-9245; Fax: +82-2-2298-8231; E-mail: thkim@hanyang.ac.kr
#These authors contributed equally to this work.

https://doi.org/10.5483/BMBRep.2024-0155

Received 9 October 2024, Revised 20 November 2024, Accepted 10 December 2024, Published online 13 January 2025

Keywords: Ankylosing spondylitis, Curdlan-injected SKG mice, Osteoclast, Pathological bone features, Wnt5a

ISSN: 1976-670X (electronic edition)

suggest that Wnt5a may be a key factor in the mediation of pathological bone erosion in rheumatoid arthritis. However, the role of Wnt5a in AS remains incompletely understood.

The SKG mouse is a BALB/c background strain carrying the W163C mutation in the Zap70 gene. The mutation in Zap70 impairs thymic selection, leading to the development of numerous highly self-reactive T cells. β-glucan injection to SKG mice activates self-reactive T cells, following predominantly differentiation into Th17 cells. These Pathological Th17 cells migrate to distal joints, playing a pivotal role in the onset and progression of chronic inflammatory arthritis. Curdlan-injected SKG mice exhibit diverse disease phenotypes including peripheral arthritis, spondylitis, ileitis, inflammatory skin disease, and uveitis. Initially, the SKG mice were reported as a model for autoimmune arthritis resembling human rheumatoid arthritis (RA). Recently, the curdlan-injected SKG mice model is more commonly applied to AS because of pathological Th17 cells considered as a therapeutic target for AS.

This paper aims to explore whether Wnt5a influences osteoclast-mediated bone resorption in curdlan-injected SKG mice that mimic AS and to provide new insights into the pathophysiological mechanisms of AS, potentially revealing new therapeutic targets.

RESULTS

An experimentally induced model mimicking pathological bone features in AS has been established, in which the injection of curdlan into SKG mice results in a dramatic increase in arthritis and significant structural bone damage. As shown in Fig. 1A, we designed an experiment to evaluate the effect of Wnt5a in a curdlan-injected SKG mouse model. Compared to the Vehicle group, the Wnt5a treatment group exhibited an increase in arthritis scores and hindpaw thickness (Fig. 1B, C). MicroCT analysis revealed that inflamed bone density in the foot was significantly greater in the Wnt5a treatment group compared to that in the Vehicle group (Fig. 1D). Additionally, ectopic bone density in the ankle measured via microCT was observed in the Wnt5a group (Fig. 1E). Histological analysis of the ankle also showed that histological scores were significantly elevated in the Wnt5a group compared to the Vehicle group (Fig. 1F). These findings indicate that the Wnt5a treatment group experienced pronounced structural changes in the bone architecture of the ankle and foot, including increased inflamed bone density and pathological bone features, in a curdlan-injected SKG mouse model.

In the Wnt5a group of curdlan-injected SKG mice, we also observed noticeable trabecular bone loss in the femur compared to the Vehicle group (Fig. 2A). Quantitative microCT measurement revealed that trabecular volume (BV/TV), trabecular thickness (Tb.Th), and trabecular number (Tb.N) were markedly reduced but trabecular separation was increased in the Wnt5a group, respectively, compared to in the Vehicle group (Fig. 2B). The serum levels of CTX-1 as bone catabolic marker and N-terminal PINP as bone anabolic marker were assessed

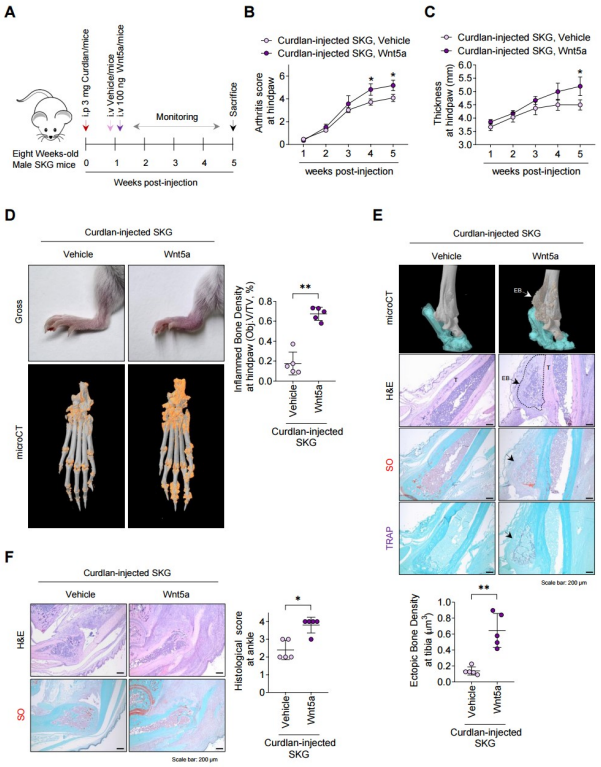

Fig. 1. Treatment with WNT5A aggravates inflammation and pathological bone features in curdlan-injected SKG mice *in vivo*. Curdlan-administered SKG mice were intravenously injected with either vehicle or 100 μg of recombinant Wnt5a and observed for up to 5 weeks (n = 5 mice per group). (A) Experimental design. (B and C) Clinical arthritis scores and hindpaw thickness were measured. (D) Representative gross images (upper) and microCT images (lower) of each group, with orange coloration indicating inflamed bone in the hindpaw. (E) Representative images taken at 5 weeks, including microCT (upper), H&E and safranin O staining (middle), and TRAP staining (lower) in the ankle. White and black arrows indicate ectopic bone formation in the tibia. (F) Histopathological assessment of the ankle was performed using a scoring method for each group. H&E, Hematoxylin & Eosin; SO, Safranin O; EB, Ectopic bone; T, Tibia. Values are expressed as mean ± SEM. *P < 0.05, **P < 0.01 by Mann–Whitney *U* test.

in collected serum. Although the PINP level did not differ between the groups, the CTX-1 serum level was significantly elevated in the Wnt5a group (Fig. 2C). Consistent with microCT data, TRAP staining confirmed an increased number of osteoclasts per tissue area in the trabecular bone of femurs in the Wnt5a group (Fig. 2D). Furthermore, bone marrow-derived OCP culture with mouse M-CSF and RANKL revealed a significantly greater number of TRAP-positive osteoclasts in the Wnt5a group compared to the Vehicle group (Fig. 2E). In line with the findings shown in Fig. 2E, the expressions of osteoclast-differentiation markers like *Itgb3*, *Dcstamp*, *Nfatc1*, and *Ctsk* (with the exception of *Acp5*) were statistically upre-

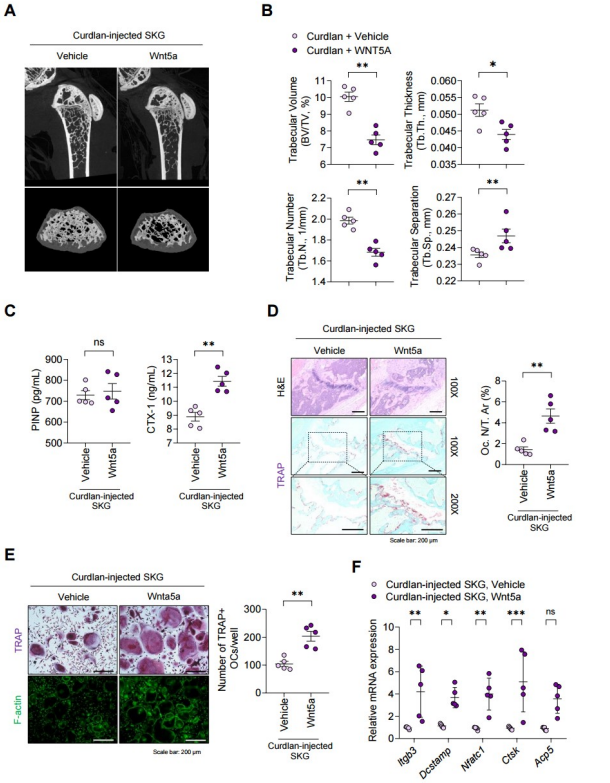

Fig. 2. Treatment with Wnt5a facilitated an increase in osteoclast activity and trabecular bone loss of curdlan-injected SKG mice *in vivo*. The Vehicle and Wnt5a-treated groups were analyzed using the following: (A) representative microCT images of femurs from each group; (B) quantitative microCT data, including trabecular volume (BV/TV), trabecular thickness (Tb.Th), trabecular number (Tb.N), and trabecular separation; (C) ELISA measurements of PINP (bone formation marker) and CTX-1 (bone resorption marker); and (D) representative H&E and TRAP staining images of femurs, alongside quantification of TRAP-positive areas. Osteoclast differentiation of bone marrow–derived OCPs from SKG mice was assessed via (E) TRAP and F-actin staining and (F) osteoclast-differentiation markers like *Itgb3, Dcstamp, Nfatc1, Ctsk,* and *Acp5*. Values are expressed as mean ± SEM. *P < 0.05, **P < 0.01 by Mann–Whitney *U* test.

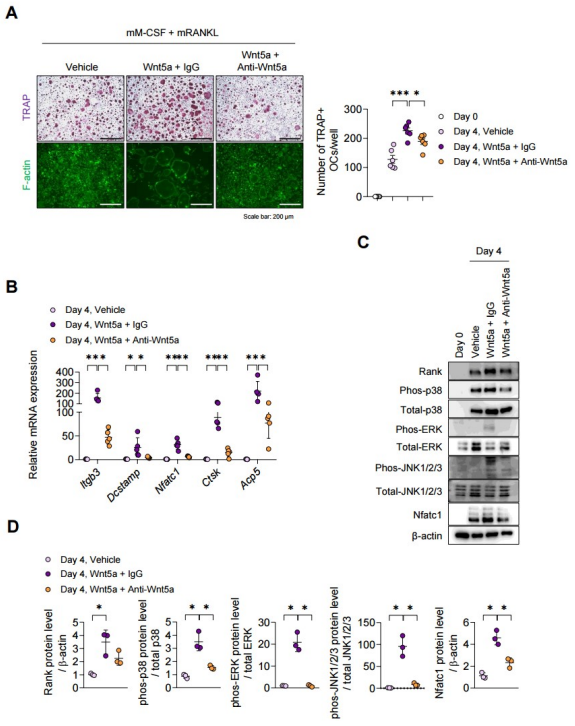

Fig. 3. Wnt5a regulates osteoclast differentiation of OCPs through activation of the Rank/p38/Nfatc1 *in vitro*. OCPs from SKG mice were differentiated with IgG or anti-WNT5A in the presence or absence of Wnt5a. At 4 days, the cells were analyzed by (A) TRAP and F-actin staining (left) and quantification of TRAP-positive cells per well (right). (B) RT-qPCR for osteoclast-differentiation markers, including *Itgb3, Dcstamp, Nfatc1, Ctsk*, and *Acp5*, and (C) immunoblotting for concentrations of osteoclast-related Rank, phos-p38, total-p38, and Nfatc1, were also performed. (D) Immunoblotting images were quantified using Image J. Values are expressed as mean ± standard deviation. *P < 0.05, **P < 0.01, ***P < 0.001 by One-Way ANOVA.

gulated in the Wnt5a group compared to the Vehicle group (Fig. 2F). These findings indicate that Wnt5a treatment promotes bone-resorbing activity by osteoclasts in the femur and osteoclast differentiation in curdlan-injected SKG mice.

To validate the observation *in vivo* that Wnt5a promotes osteoclast differentiation, we conducted an *in vitro* experiment using OCPs of SKG mice. OCPs from SKG mice were treated with Wnt5a and/or anti-Wnt5a under osteoclast induction with mouse M-CSF and RANKL, and osteoclast differentiation was assessed using TRAP staining. Interestingly, Wnt5a treatment promoted osteoclast differentiation compared to vehicle, whereas anti-Wnt5a treatment hindered the osteoclast response by Wnt5a (Fig. 3A). Moreover, upregulation of osteoclast-differentiation markers by Wnt5a was significantly reduced in the anti-Wnt5a group (Fig. 3B). Consistent with these findings, we confirmed by immunoblotting that protein levels of Rank, phos-p38, phos-ERK, phos-JNK, and Nfact1 were up- and down-regulated in Wnt5a and/or anti- Wnt5a (Fig. 3C). Thus, we conclude that Wnt5a plays a regulatory role in osteoclast differentiation of OCPs from SKG mice.

DISCUSSION

Briolay *et al.* (8) demonstrated that Tumor necrosis factor alpha (TNFa) promotes osteoblast differentiation and mineralization of human mesenchymal stem cells through activating Wnt5a expression. Similarly, Li *et al.* (6) reported that TNFa stimulates Wnt5a expression in monocytes and macrophages in a dose- and time-dependent manner. Moreover, Wnt5a expression was highly enriched in surgical tissues of patient with AS. Thus,

these data indicate a strong association between TNFa and Wnt5a expression, shedding light on their role in influencing inflammation-mediated new bone formation in AS.

Wnt signaling involves a canonical pathway and a non-canonical pathway, and Wnt molecules are well-known for their role in development, tissue homeostasis, and various diseases (9, 10). In general, the canonical Wnt signaling pathway promotes target genes through β-catenin, while the non-canonical pathway operates it through RhoA, JNK, and PKC, altering intracellular calcium levels or activating other transcription factors to induce cellular responses. Wnt research has predominantly focused on the canonical pathway. However, in the case of Wnt5a, there has been a notable emphasis on its role in the non-canonical pathway, distinguishing it from other Wnt proteins in various disease or animal models (11-15). Treatment with BMP2 drives osteoblast differentiation by activating the Wnt5a/ROR2 signaling pathway, supporting the idea that the BMP2/Wnt5a/ROR2 signaling pathway has substantial importance in osteoblast differentiation (16). Furthermore, Wnt signaling governs pathological bone formation in AS (17, 18). While the effects of Wnt5a on osteoblasts and bone formation in AS have been reported, its impact on osteoclasts has yet to be investigated.

As shown in Fig. 3, treatment with Wnt5a exhibits enhancement of osteoclast activity. Notably, Wnt5a induces Rank, phos-p38, phos-ERK, phos-JNK and Nfact1 protein expressions in osteoclasts of SKG mice, while anti-Wnt5a attenuates this induction (Fig. 3C). Moreover, blockade of Wnt5a attenuates arthritis and osteoclast differentiation, indicating that Wnt5a is a promising therapeutic target for inflammation and bone erosion in RA (7, 19). Since Ror2 expression was significantly elevated in bone marrow cells from curdlan-injected SKG mice compared to PBS injection as control (Supplementary Fig. 1), it is reasonable to speculate that Ror2 may contribute to the osteoclast differentiation. Furthermore, the association of Wnt5a-Ror2 signaling with osteoclast differentiation and activity is consistent with previous finding (7). Therefore, Wnt5a and Ror2 plays a critical role as a regulator of bone resorption or inflamed-mediated bone loss in both RA and AS.

The involvement of Wnt5a in new bone formation of AS had been reported. We treated human osteoprogenitor cells with recombinant Wnt5a to observe osteoblast activity. Contrary to previous reports and expectations, Wnt5a did not have a significant effect on osteoblast differentiation of osteoprogenitor cells (Supplmentary Fig. 2). This may be due to insufficient stimulation by Wnt5a or possibly influenced by the inflammatory condition present in patients with AS. Furthermore, we previously conducted studies on the role of osteoclasts and macrophages in the pathogenesis of AS (20, 21), revealing that osteoclasts at inflammatory sites not only exhibit increased bone resorption activity but also secrete elevated levels of platelet-derived growth factor B, which was highly conserved in serum and pathological tissues of AS. The secreted proteins from Wnt5a-stimulated osteoclasts that may stimulate osteoblasts require further study.

ZAP-70, a critical signaling molecule in T cells, plays a pivotal role in the pathogenesis of autoimmune diseases, including AS. In the SKG mouse model, the ZAP-70 mutation leads to chronic inflammation and subsequent bone destruction, mimicking key features of AS (22). Wnt5a, derived from preosteoblasts, is a potent stimulator of osteoclast differentiation (7). It is upregulated under inflammatory conditions and serves as a key mediator linking inflammation to bone erosion. The interplay between ZAP-70 and Wnt5a can be understood in the context of immune-mediated bone destruction: ZAP-70-driven inflammation enhances the production of inflammatory cytokines such as TNF, which in turn promote Wnt5a expression (8). Wnt5a subsequently promotes osteoclast differentiation and activation, exacerbating bone erosion in AS. Thus, ZAP-70, Wnt5a, and osteoclast differentiation are interconnected through a shared inflammatory signaling axis that drives pathological bone resorption in AS.

In conclusion, Wnt5a treatment accelerated inflammation, structural bone damage, and trabecular bone loss in curdlan-injected SKG mice compared to vehicle-treated mice. Osteoclast activity was significantly greater in the Wnt5a-treated group of curdlan-injected SKG mice than in the Vehicle group. Moreover, Wnt5a promoted osteoclast differentiation of OCPs from SKG mice, while anti-Wnt5a treatment mitigated osteoclast differentiation. Therefore, Wnt5a may represent a potential therapeutic target to prevent pathological bone features in AS.

MATERIALS AND METHODS

Curdlan-injected SKG mice

All experimental procedures were carried out according to the Guide for the Care and Use of Laboratory Animals and received approval from the Animal Ethics Screening Committee at Hanyang University (2023-0116A). SKG mice, which exhibit a ZAP-70 mutation and are derived from the BALB/c strain, were initially acquired from Dr. Sakaguchi at Osaka University, Suita, Japan (23). A total of 10 eight-week-old male SKG mice were intraperitoneally administered 3 mg of curdlan (0.30-09903; Wako Chemical, Osaka, Japan). The mice were subsequently divided randomly into two groups (five mice per group). After 1 week, one group was given PBS injections as a vehicle control, while the other group received 100 μg of human/mouse recombinant Wnt5a (645-WN; R&D Systems, Minneapolis, MN, USA) via injection and was monitored for an additional 5 weeks.

All mice were monitored for a duration of up to 5 weeks, and assessments were conducted by two blinded observers using the following scoring criteria: 0 = no swelling or redness of digits, 0.1 = swelling or redness of the digits, 0.5 = mild swelling and/or redness of the wrists or ankle joints, and 1 = severe swelling of the larger joints. The scores for the affected joints were summed, with a maximum possible score of 6 points (22).

Histological analysis

Ankle joint tissues from each group were fixed in 10% formalin for 1 week and then decalcified in 14% Ethylenediaminetetraacetic acid (EDTA) buffer for 7 days, embedded in paraffin, and sectioned into 5-μm-thick slices. The staining procedures were conducted following the standard protocols or the manufacturer's instructions. The slides underwent hematoxylin (1.05174.0500; Merck, Kenilworth, NJ, USA) and eosin (H&E) staining for histological analysis and safranin O (146 640250; Thermo Fisher Scientific, Waltham, MA, USA)/fast green (F7252; Sigma-Aldrich, St. Louis, MO, USA) (SOFG) staining for cartilage observation, and tartrate-resistant acid phosphatase (TRAP) staining was performed using a commercially available TRAP kit (PMC-AK04F; Cosmo Bio). All slides were mounted with a permanent mounting medium (H-5000; Vector Laboratories, Burlingame, CA, USA). The histopathological score was performed using H&E and safranin O staining. Histopathological features of the mouse ankles were scored on a scale of 1−4 points, as follows: 1 = few infiltrating immune cells, 2 = small patches of inflammation, 3 = inflammation throughout the ankle joint, and 4 = inflammation in soft tissues/entheses/fasciitis (22).

Micro–computed tomography (microCT)

MicroCT imaging was performed to collect data, which were processed at the 2nd Analysis Lab in Seoul, Korea. Mouse ankle samples were preserved in 10% formalin for 1 week and subjected to high-resolution imaging using the Skyscan1272 microCT scanner (Bruker MicroCT, Kontich, Belgium). The scanning parameters were a voltage of 60 kV with a 0.25-mm aluminum filter and a resolution of 9 μm per pixel. The collected microCT scans facilitated three-dimensional histomorphometric assessments. Image reconstruction was carried out using NRecon v1.7.3.1 and InstaRecon software, followed by analysis with CTAn v1.20.3.0 (Bruker MicroCT). The resulting three-dimensional visualizations were generated with CTVol v2.3.2.0 (Bruker MicroCT).

Isolation of bone marrow–derived osteoclast precursor cells (OCPs) and osteoclast differentiation

Murine OCP isolation and osteoclast differentiation were performed as previously described (24-26). Bone marrow was flushed out of the femur and tibia with alpha-MEM (LM008-53; Welgene) supplemented with 10% FBS (16000044; Gibco, Gaithersburg, MD, USA) and 1% penicillin–streptomycin (151 40122; Gibco) using a 23-gauge needle. Bone marrow cells were treated with ACK lysis buffer (A10492-01; Gibco) and washed with complete alpha-MEM. Bone marrow was cultured with complete alpha-MEM in the presence of 10 ng/ml of M-CSF (315-02; PeproTech) for 1 day, and monocyte cells were collected in a suspension. Additionally, suspended monocyte cells were cultured with 20 ng/ml of M-CSF for 1 day to generate mouse OCPs, which were subsequently incubated with 50 ng/ml of M-CSF and 100 ng/ml of RANKL (315-11C; PeproTech) for additional 4 days depending on the experiment. The culture medium was changed at 3 days. TRAP-positive osteoclasts were stained with a TRAP kit (PMC-AK04F; Cosmo) and counted. Human/mouse recombinant Wnt5a (645-WN; R&D Systems) and anti-Wnt5a (MAB645; R&D Systems) were used for stimulation and neutralization, respectively.

RT-qPCR and immunoblotting

Total mRNA and protein extractions were conducted as previously described (20, 21). In summary, total RNA was isolated using Trizol (15596018; Thermo Fisher Scientific), while cDNA was synthesized with reverse transcriptase (EP0441; Thermo Fisher Scientific) using a thermal cycler (T100; Bio-Rad Laboratories, Hercules, CA, USA). This was followed by PCR using the CFX Duet real-time PCR system (Bio-Rad Laboratories). The mRNA levels of the target genes were quantified and normalized to those of GAPDH. The primers used for RT-qPCR are listed in Table 1.

The total protein of cells was extracted by RIPA buffer, including protease (P9599; Sigma-Aldrich) and phosphatase inhibitors (5870S; Cell Signaling Technology, Danvers, CA, USA), and quantified with the Bradford protein assay kit (23200; Thermo Fisher Scientific). The proteins (40 μg) were loaded onto 10 or 12.5% SDS-PAGE and transferred to nitrocellulose membranes (10600003; Cytiva). The membranes were then blocked in 5% non-fat milk for 1 h at room temperature. The primary antibodies were incubated overnight at 4°C. Nfatc1 (1:1000, 556602; BD Biosciences, Franklin Lakes, NJ, USA), phospho-p38 (1:1000, 9215; Cell Signaling Technology), total p38 (1:1000, sc-535; Santa Cruz Biotechnology, Dallas, TX, USA), Rank (1:1000, sc-374360; Santa Cruz Biotechnology), and β-actin (1:1000, 4970; Cell Signaling Technology)

Table 1. RT-qPCR primer sequences

Gene	Forward	Reverse
Gapdh	TCCTGTAGTAGCAGCCCCTT	CAGCAAGCTCAAAGGGCAAG
Ctsk	TGGAGGCGGCTATATGACCA	CCTTTGCCGTGGCGTTATAC
Itgb3	GAAACAGAGCGTGTCCCGTA	GGTCTTGGCATCCGTGGTAA
Acp5	TGGCTTTGCCTATGTGGA	CCTGGTCTTAAAGAGGGACTT
Dcstamp	AAAGCTTGCCAGGGTTTGAG	GGTTTTGGGATACAGTTGGGTTC

were used as primary antibodies. Secondary mouse (115-035-003; Jackson Immunoresearch, Grove, PA, USA) and rabbit (111-035-003, Jackson Immunoresearch) antibodies were used. Immunoblotting was detected using ChemiDoc (Alliance Mini HD9; UVITEC) with West Pico PLUS chemiluminescent substrate (34580; Thermo Fisher Scientific).

Enzyme-linked immunosorbent assay (ELISA)

The mouse was anesthetized, and blood was collected in a blood-collection tube (BD-119497; BD Biosciences) via cardiac puncture using an insulin syringe. Blood was maintained at room temperature for 1 h, then centrifuged at 1,500 rpm for 20 min. The supernatant was collected and stored at -80^{o}C. C-terminal telopeptide of type 1 collagen (CTX-1) and N-terminal propeptide of type I procollagen (PINP) were used bone catabolic marker and bone anabolic marker, respectively. ELISA assay for PINP (CSB-E12775m; CUSABIO), and CTX-1 (CSB-E12782m; CUSABIO) were carried out following the manufacturer's instructions.

Isolation and osteogenic differentiation of human osteoprogenitor cells

This study was approved by the Institutional Review Board of Hanyang University Seoul Hospital (IRB No. 2014-05-001). The human osteoprogenitor derived from bone chips were induced with osteogenic differentiation into matrix maturation and mineralization. More details about isolation of osteoprogenitor cells, differentiation into osteoblasts, and assessment kits for matrix maturation and mineralization were previously addressed (27). Osteoprogenitor cells were confirmed the absence of mycoplasma contamination before subsequent experiments. For osteogenic differentiation, primary osteoprogenitor cells were cultured in an induction medium containing 50 μM ascorbic acid (Sigma-Aldrich, MO, USA), 10 mM β-glycerophosphate (Santa Cruz, TX, USA), and 100 nM dexamethasone (Sigma-Aldrich). The differentiation medium was changed every three days. To assess matrix maturation and mineralization, cells were subjected to alkaline phosphatase (ALP) activity and staining with alizarin red (ARS), von Kossa (VON), and hydroxyapatite (HA).

Statistical analysis

Statistical analyses were performed using the Mann–Whitney *U* test for comparisons between two groups. For comparisons among three groups, one-way analysis of variance was completed. All statistical tests, including the Mann–Whitney *U* test and one-way analysis of variance, were conducted using GraphPad Prism 10 (GraphPad Software, La Jolla, CA, USA). Data are presented as mean ± standard error of the mean (SEM) values. All experiments were performed at least three times. Statistical significance is indicated by asterisks, with $*P < 0.05$, $**P < 0.01$, and $***P < 0.001$.

ACKNOWLEDGEMENTS

This work was supported by the Soonchunhyang University Research Fund and the Basic Science Research Program through the National Research Foundation of Korea (2021R1A6A1A03038899, 2021R1A6A1A03039503, and RS-2024-00351695). DEG analysis of RNA-seq data required during revision was performed by Soonchunhyang University (Z-202212203727, National research Facilities and Equipment Center).

CONFLICTS OF INTEREST

The authors have no conflicting interests.

REFERENCES

1. Braun J and Sieper J (2007) Ankylosing spondylitis. Lancet 369, 1379-1390
2. Dougados M and Baeten D (2011) Spondyloarthritis. Lancet 377, 2127-2137
3. Tam LS, Gu J and Yu D (2010) Pathogenesis of ankylosing spondylitis. Nat Rev Rheumatol 6, 399-405
4. Carter S, Braem K and Lories RJ (2012) The role of bone morphogenetic proteins in ankylosing spondylitis. Ther Adv Musculoskelet Dis 4, 293-299
5. Lories RJ, Luyten FP and de Vlam K (2009) Progress in spondylarthritis. Mechanisms of new bone formation in spondyloarthritis. Arthritis Res Ther 11, 221
6. Li X, Wang J, Zhan Z et al (2018) Inflammation intensity-dependent expression of osteoinductive Wnt proteins is critical for ectopic new bone formation in ankylosing spondylitis. Arthritis Rheumatol 70, 1056-1070
7. Maeda K, Kobayashi Y, Udagawa N et al (2012) Wnt5a-Ror2 signaling between osteoblast-lineage cells and osteoclast precursors enhances osteoclastogenesis. Nat Med 18, 405-412
8. Briolay A, Lencel P, Bessueille L, Caverzasio J, Buchet R and Magne D (2013) Autocrine stimulation of osteoblast activity by Wnt5a in response to TNF-alpha in human mesenchymal stem cells. Biochem Biophys Res Commun 430, 1072-1077
9. Clevers H and Nusse R (2012) Wnt/beta-catenin signaling and disease. Cell 149, 1192-1205
10. Clevers H (2006) Wnt/beta-catenin signaling in development and disease. Cell 127, 469-480
11. El Zouka Y, Sheta E, Abdelrazek Salama M, Selima E, Refaat R and Salaheldin Abdelhamid Ibrahim S (2024) Tetrandrine ameliorated atherosclerosis in vitamin D3/high cholesterol diet-challenged rats via modulation of miR-34a and Wnt5a/Ror2/ABCA1/NF-kB trajectory. Sci Rep 14, 21371
12. Chen Z, Zhong W, Zhang R, Li G, Zhang Y and Zhang M (2024) Down-regulation of PCBP2 suppresses the invasion and migration of trophoblasts via the WNT5A/ROR2 pathway in preeclampsia. Biol Reprod 111, 1142-1155
13. Grither WR, Baker B, Morikis VA, Ilagan MXG, Fuh KC and Longmore GD (2024) ROR2/Wnt5a signaling regulates directional cell migration and early tumor cell invasion in ovarian cancer. Mol Cancer Res 22, 495-507

14. Zhang CJ, Zhu N, Liu Z et al (2020) Wnt5a/Ror2 pathway contributes to the regulation of cholesterol homeostasis and inflammatory response in atherosclerosis. Biochim Biophys Acta Mol Cell Biol Lipids 1865, 158547
15. Feike AC, Rachor K, Gentzel M and Schambony A (2010) Wnt5a/Ror2-induced upregulation of xPAPC requires xShcA. Biochem Biophys Res Commun 400, 500-506
16. Nemoto E, Ebe Y, Kanaya S et al (2012) Wnt5a signaling is a substantial constituent in bone morphogenetic protein-2-mediated osteoblastogenesis. Biochem Biophys Res Commun 422, 627-632
17. Corr M (2014) Wnt signaling in ankylosing spondylitis. Clin Rheumatol 33, 759-762
18. Zeng Y, Wang T, Liu Y et al (2022) Wnt and Smad signaling pathways synergistically regulated the osteogenic differentiation of fibroblasts in ankylosing spondylitis. Tissue Cell 77, 101852
19. Huang Y, Xue Q, Chang J, Wang X and Miao C (2023) Wnt5a: a promising therapeutic target for inflammation, especially rheumatoid arthritis. Cytokine 172, 156381
20. Jo S, Lee JS, Nam B et al (2022) SOX9(+) enthesis cells are associated with spinal ankylosis in ankylosing spondylitis. Osteoarthr Cartil 30, 280-290
21. Jo S, Lee SH, Park J et al (2023) Platelet-derived growth factor B is a key element in the pathological bone formation of ankylosing spondylitis. J Bone Miner Res 38, 300-312
22. Ruutu M, Thomas G, Steck R et al (2012) Beta-glucan triggers spondylarthritis and Crohn's disease-like ileitis in SKG mice. Arthritis Rheum 64, 2211-2222
23. Sakaguchi N, Takahashi T, Hata H et al (2003) Altered thymic T-cell selection due to a mutation of the ZAP-70 gene causes autoimmune arthritis in mice. Nature 426, 454-460
24. Oh Y, Park R, Kim SY et al (2021) B7-H3 regulates osteoclast differentiation via type I interferon-dependent IDO induction. Cell Death Dis 12, 971
25. Piao X, Kim JW, Hyun M et al (2023) Boeravinone B, a natural rotenoid, inhibits osteoclast differentiation through modulating NF-kappaB, MAPK and PI3K/Akt signaling pathways. BMB Rep 56, 545-550
26. Lee SH, Park SY, Kim JH, Kim N and Lee J (2023) Ginsenoside Rg2 inhibits osteoclastogenesis by downregulating the NFATc1, c-Fos, and MAPK pathways. BMB Rep 56, 551-556
27. Jo S, Lee SH, Jeon C et al (2023) Elevated BMPR2 expression amplifies osteoblast differentiation in ankylosing spondylitis. J Rheum Dis 30, 243-250